Drug Design, Development and Therapy

Dovepress
open access to scientific and medical research

Open Access Full Text Article

ORIGINAL RESEARCH

α-Mangostin from *Cratoxylum arborescens* demonstrates apoptogenesis in MCF-7 with regulation of NF-κB and Hsp70 protein modulation in vitro, and tumor reduction in vivo

This article was published in the following Dove Press journal:
Drug Design, Development and Therapy
27 September 2014
Number of times this article has been viewed

Mohamed Yousif Ibrahim[1]
Najihah Mohd Hashim[1]
Syam Mohan[2]
Mahmood Ameen Abdulla[3]
Behnam Kamalidehghan[1]
Mostafa Ghaderian[1,4]
Firouzeh Dehghan[1,5]
Landa Zeenelabdin Ali[1]
Ismail Adam Arbab[6]
Maizatulakmal Yahayu[7]
Gwendoline Ee Cheng Lian[8]
Fatemeh Ahmadipour[1]
Hapipah Mohd Ali[9]

[1]Department of Pharmacy, Faculty of Medicine, University of Malaya, Kuala Lumpur, Malaysia; [2]Medical Research Centre, Jazan University, Jazan, Saudi Arabia; [3]Department of Molecular Medicine, Faculty of Medicine University of Malaya, Kuala Lumpur, Malaysia; [4]Epigenetics Lab, Institute of Biological Sciences, Faculty of Science, University of Malaya, Kuala Lumpur, Malaysia; [5]Department of Physiology, Faculty of Medicine, University of Malaya, Kuala Lumpur, Malaysia; [6]School of Chemical Sciences and Food Technology, Faculty of Science and Technology, Universiti Kebangsaan Malaysia, Selangor, Malaysia; [7]Department of Bioproduct Research and Innovation, Institute of Bioproduct Development (IBD), Universiti Teknologi Malaysia, Johor, Malaysia; [8]Department of Chemistry, Faculty of Science, Universiti Putra Malaysia, Selangor, Malaysia; [9]Department of Chemistry, University of Malaya, Kuala Lumpur, Malaysia

Correspondence: Najihah Mohd Hashim
Department of Pharmacy, Faculty of Medicine, University of Malaya, 50603 Kuala Lumpur, Malaysia
Tel +60 1 2327 9594
Fax +60 3 7967 4964
Email najihahmh@um.edu.my

Mohamed Yousif Ibrahim
Department of Pharmacy, Faculty of Medicine, University of Malaya, 50603 Kuala Lumpur, Malaysia
Tel +60 1 7337 9596
Fax +60 3 7967 4964
Email al_omdah2003@hotmail.com

Abstract: *Cratoxylum arborescens* is an equatorial plant belonging to the family Guttiferae. In the current study, α-Mangostin (AM) was isolated and its cell death mechanism was studied. HCS was undertaken to detect the nuclear condensation, mitochondrial membrane potential, cell permeability, and the release of cytochrome c. An investigation for reactive oxygen species formation was conducted using fluorescent analysis. To determine the mechanism of cell death, human apoptosis proteome profiler assay was conducted. In addition, using immunofluorescence and immunoblotting, the levels of Bcl-2-associated X protein (Bax) and B-cell lymphoma (Bcl)-2 proteins were also tested. Caspaces such as 3/7, 8, and 9 were assessed during treatment. Using HCS and Western blot, the contribution of nuclear factor kappa-B (NF-κB) was investigated. AM had showed a selective cytotoxicity toward the cancer cells with no toxicity toward the normal cells even at 30 μg/mL, thereby indicating that AM has the attributes to induce cell death in tumor cells. The treatment of MCF-7 cells with AM prompted apoptosis with cell death-transducing signals. This regulated the mitochondrial membrane potential by down-regulation of Bcl-2 and up-regulation of Bax, thereby causing the release of cytochrome c from the mitochondria into the cytosol. The liberation of cytochrome c activated caspace-9, which, in turn, activated the downstream executioner caspace-3/7 with the cleaved poly (ADP-ribose) polymerase protein, thereby leading to apoptotic alterations. Increase of caspace 8 had showed the involvement of an extrinsic pathway. This type of apoptosis was suggested to occur through both extrinsic and intrinsic pathways and prevention of translocation of NF-κB from the cytoplasm to the nucleus. Our results revealed AM prompt apoptosis of MCF-7 cells through NF-κB, Bax/Bcl-2 and heat shock protein 70 modulation with the contribution of caspaces. Moreover, ingestion of AM at (30 and 60 mg/kg) significantly reduced tumor size in an animal model of breast cancer. Our results suggest that AM is a potentially useful agent for the treatment of breast cancer.

Keywords: α-Mangostin, apoptosis, mitochondria, protein array, caspace 3/7, NF-κB

Introduction

Breast cancer is one of the most deadly cancers affecting women worldwide because of its high rate of incidence and mortality. According to the American Cancer Society, breast cancer is emphasized to account for 26% of all new cancer cases, which is the highest in percentage among all the cancers in American women.[1] In Malaysia, the National Cancer Registry reported that one in 20 Malaysian women are at a risk of acquiring breast cancer in their lifetime.[2] This incidence rate is still considered low

compared to one in eight women in Europe and the United States.[3] The causes, due to which up to 70% of breast cancer development occurs in women, are reported to be of environmental factors and lifestyle. The remaining 30% may be attributed to genetic factors.[4,5]

Among the cancer treatment strategies, use of radiation therapy became a valuable tool for the control of local and regional diseases after 1960 with the invention of the linear accelerator, but, like surgery, radiation therapy alone could not enucleate metastatic cancer. Nevertheless, the success of the treatment depends on the capacity to reach every organ in the body of patients. Drugs, biological molecules, and immune-mediated remedies have therefore become the focus in the current efforts to cure cancer. Chemotherapy is defined as a mode of treatment in which drugs are used to retard or destroy the growth of malignant cells. These drugs are either used alone or in combination with one or more other drugs. For many years, tamoxifen has been considered as the drug of choice for the cure of estrogen-dependent cases. The antitumor effect of tamoxifen is due to the arrest of growth and prompting apoptosis,[6] which is mediated by linkage to the intracellular estrogen receptor on the breast cancer cells, blocking of steroid hormone action,[7] inhibition of protein kinase C[8] and its binding to calmodulin.[9]

However, there are various side effects like development of liver cancer, increased blood clotting, retinopathy, and corneal opacities when performing chemotherapy with tamoxifen.[10] Due to these side effects, the use of herbs as an alternative therapy has attracted a great deal of interest by virtue of the lower toxicity and cost benefits.[11] Many clinical attempts using herbs or natural products are being conducted around the world.[12] Furthermore, some herbs and their constituents have been reported to suppress the proliferation of cancer cells directly. Thus, the use of herbs could be a more effective strategy in the cure of cancer.[13]

Cratoxylum arborescens (*C. arborescens*) Blume is a traditional herb belonging to the Guttiferae family, and its natural range of distribution includes Malaysia, South Burma, Sumatra, and Borneo.[14] This plant is used traditionally as a cure for fever, cough, diarrhea, and other ailments.[15] The phytochemicals found in *C. arborescens* include a pharmacologically superior class of phytochemicals, xanthones.[14,16] α-Mangostin (AM) (Figure 1A) is one of the major xanthones extracted from the stem bark of this plant.[17] AM possesses a wide spectrum of biological activities, which includes anti-inflammatory,[18,19] cardioprotective,[20] antitumor,[21,22] anti-diabetic,[23] antibacterial,[24] antifungal,[25] antioxidant,[18,26] anti-parasitic,[27] and anti-obesity[28] properties.

In this study, we evaluated the apoptotic cell death mechanism prompted by AM on breast cancer using MCF-7 cells as an in vitro model. In addition to that, we investigated the antitumor activity of AM in the animal model.

Materials and methods

Cell culture

Normal breast cells, MCF-10 A, and MCF-7 cells, were acquired from the American Type Culture Collection (Manassas, VA, USA) and then kept at 37°C in an incubator with 5% CO_2 saturation. They were grown in Roswell Park Memorial Institute medium (RPMI)-1640 (PAA Laboratories GmbH, Coelbe, Germany) together with 10% Fetal Bovine Serum (FBS).

Anti-proliferative effect of AM on MCF-7 cells

The inhibitory effect of AM was determined by MTT assay, in which 1×10^5 of MCF-7 cells/μL were seeded in triplicate in 96-well plates and kept for 24 hours at 37°C with 5% CO_2 saturation. After 24 hours' incubation, a serial dilution for different concentrations of AM was prepared and transferred to the MCF-7 cells and incubated for 24 hours in 37°C and 5% CO_2; 20 μL of 3-[4,5-dimethylthiazol-2-yl]-2,5-diphenyltetrazolium bromide (MTT solution, 5 mg/mL) was added to the treated cells in a dark place, covered with foil, and incubated for 4 hours. All media were discharged and a total of 100 μL volume of dimethyl sulfoxide was poured into each well until the purple formazan crystals dissolved. The plate was measured using a microplate reader (Tecan Group Ltd., Männedorf, Switzerland) at absorbance 570 nm. The experiment was conducted in triplicate to evaluate half-maximal inhibitory concentration for AM against the MCF-7 cell line.

Acridine orange propidium iodide double staining using fluorescent microscopy

MCF-7 cells were quantified using acridine orange (AO) and propidium iodide (PI) double-staining in conformity with the standard procedures, and inspected under a fluorescence microscope (Leica [Leica Microsystems, Wetzlar, Germany] with Q-Floro Software [Leica Microsystems]). Concisely, the treatment was conducted in a 25 mL culture flask, in which 1×10^5 MCF-7 cells/mL were seeded and treated with different concentrations of AM (5, 10, and 20 mg/mL) for 24 hours. After 24 hours, the cells were centrifuged at 1,800 rpm for 5 minutes to discharge the old medium; then a cool PBS was used to wash

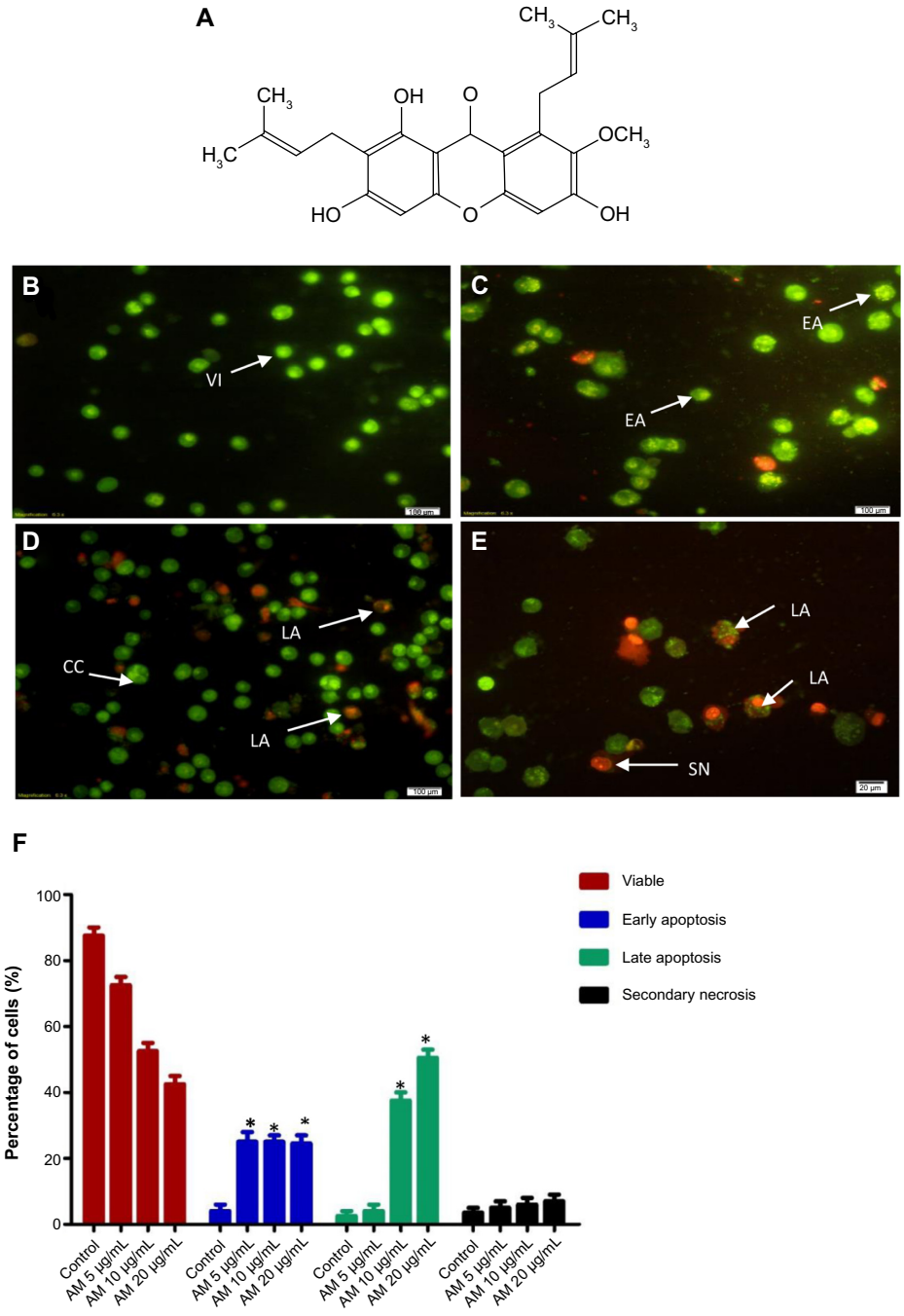

Figure 1 Chemical structure of α-Mangostin (**A**). Fluorescent micrographs of AO and PI double-stained MCF-7 cells; (**B**) untreated cells showed normal structure without prominent apoptosis and necrosis; (**C**) early apoptosis features were seen after treatment with 5 μg/mL representing intercalated acridine orange (bright green) amongst the fragmented DNA; (**D**) blebbing and orange color representing the hallmark of late apoptosis were noticed in 10 μg/mL treatment; (**E**) bright red color secondary necrosis were visible after treatment with 20 μg/mL; (**F**) percentages of viable, early apoptotic, late apoptosis and secondary necrotic cells after AM treatment. MCF-7 cell death via apoptosis increased significantly (*$P<0.05$) in a concentration-dependent manner. However, no significant ($P>0.05$) difference was observed in the cell count of necrosis.
Abbreviations: AM, α-Mangostin; AO, acridine orange; PI, propidium iodide; VI, viable cells; CC, chromatin condensation; LA, late apoptosis; EA, early apoptosis; SN, secondary necrosis.

the cells two times before staining with AO/PI. Equal amounts, 10 μL (10 μg/mL), of fresh AO and PI were prepared and covered from light to stain the cell onto a glass slide, which was covered with a cover slip. The slides were viewed under a fluorescence microscope 30 minutes prior to the fluorescence fading.

Assay of the apoptotic rate by Annexin V (AV)-fluorescein isothiocyanate (FITC) staining

MCF-7 at concentration (1×10^5 cells/mL) was exposed to 5, 10, and 20 μg/mL concentrations of AM, and the AV assay

was executed with the use of the BD Pharmingen™ Annexin V-FITC Apoptosis Detection Kit (APO Alert Annexin V, Clontech, Mountain View, CA, USA). The treated cells were centrifuged for 5 minutes at 1,800 rpm to eliminate the media. Subsequently, cells were washed with 1× binding buffer provided by the manufacturer. Then the cells were re-suspended in 200 µL of binding buffer; 5 µL of AV, and 10 µL of PI (Sigma-Aldrich Co, St Louis, MO, USA) were added before incubating at 37°C in the dark for 15 minutes. The binding buffer raised the reaction volume to 500 µL for the flow cytometric analysis. Flow cytometric analysis was conducted using FACS Canto II, (BD Biosciences, San Jose, CA, USA) cytometry b. The dimethyl sulfoxide-treated (0.1%, v/v) cells were employed as the control.

Nuclear morphology, membrane permeability, mitochondrial membrane potential Δψm (MMP), and cytochrome c release analysis

A Cellomics Multiparameter Cytotoxicity 3 Kit (Thermo Fisher Scientific, Waltham, MA, USA) was employed as previously described at length.[29] The kit facilitates concurrent measurements of six independent parameters at the same time for the same cell population. Chromatin condensation, morphological change, detection of the MMP, release of cytochrome c, and cell permeability were used to test the loss of the MCF-7 cells. MCF-7 (1×10^5 cells/mL) were used to seed in 96 wells (Genetix Biotech Asia Pvt. Ltd., New Delhi, India) and treated with AM (5, 10, and 20 mg/mL). After 24 hours, the plates were processed according to the manufacturer's instructions, and analyzed using the ArrayScan HCS system (Thermo Fisher Scientific). The images and the intensity data were reading the texture of the fluorescence inside each of the cells, together with the typical fluorescence of the cell population inside the well. The experiment was done in triplicate.

Immunofluorescence analysis of Bax/Bcl-2

A total of 5×10^3 MCF-7 cells were seeded in a 96 well plate (genetix), followed by 5, 10, and 20 µg/mL of AM treatment. Then, the cells were fixed for 15 minutes at 37°C by 4% paraformaldehyde after rinsing two times with PBS. PBS was used to rinse the cells three times, the cells were treated using a blocking buffer for 60 minutes incubation in 0.03% Triton X-100/PBS (Sigma-Aldrich, St Louis, MO, USA) and normal serum before the cells were rinsed once more with PBS. The diluted primary antibody solution containing 1× PBS/1% BSA/0.3% Triton X-100, was added after the aspirate blocking buffer. The cells underwent incubation overnight at 4°C. B-cell lymphoma (Bcl)-2 and Bcl-2-associated X protein (Bax) fluorochrome-conjugated secondary antibody diluted (Santa Cruz Biotechnology Inc., Dallas, TX, USA) in antibody dilution or in PBS only was added to the cells and incubated for 1 hour. After rinsing three times in PBS, the cells were treated with DAPI and examined using the CellReporter™ cytofluorimeter system (Molecular Devices LLC, Sunnyvale, CA, USA).

Bioluminescent assay of caspaces 3/7, 8, and 9

A concentration-dependent study of the activity of caspace-3/7, 8, and 9 was done using luminescence-based assay, Caspace-Glo™ 3/7, Caspace-Glo™ 8, and Caspace-Glo™ 9 Assay (Promega Corporation, Fitchburg, WI, USA). The cells were seeded in 96-well plates in 50 µL of RPMI 1640 together with 10% FBS and incubated for 24 hours. Then, the cells were treated with AM 5, 10, and 20 µg/mL and incubated for 24 hours at 37°C with 5% CO_2. After 24 hours, 100 µL of the assay reagent was added and the plate was incubated for 1 hour at 37°C. Luminescence was calculated using a Tecan Infinite®200 Pro (Tecan, Männedorf, Switzerland) microplate reader.

Western blot analysis

MCF-7 cells were cultured in a 25 mL flask (TPP Techno Plastic Products AG, Trasadingen, Switzerland) and treated with AM 5, 10, and 20 µg/mL. The cells were collected, washed by cool PBS, and mixed with a lysis buffer (50 mM Tris-Hcl pH 8.0, 120 mM NaCl, 0.5% NP-40, 1 mM phenylmethylsulfonyl fluoride) to isolate the total proteins from the cells. A 40 µg measure of the extracted protein was separated using 12% sodium dodecyl sulphate-polyacrylamide gel electrophoresis, then moved to a polyvinylidene difluoride membrane (Bio-Rad Laboratories Inc., Hercules, CA, USA), and blocked with 5% non-fat milk in a TBS-Tween buffer 7 (0.12 M Tris-base, 1.5 M NaCl, 0.1% Tween 20) for 30 minutes at room temperature, and incubated with the appropriate primary antibody overnight at 4°C, then incubated with alkaline phosphatase-conjugated secondary antibody for 30 minutes at room temperature, and then washed in Tris-buffered saline and Tween 20 buffer. The primary antibodies, β-actin (sc-130300), Bax (sc-20067), heat shock protein (Hsp)70 (sc-69705), proliferating cell nuclear antigen (PCNA) (sc-25280), Nf-κB/P65 (sc-398442), cytochrome c (sc-13560), caspace-7 (sc-

81660), caspace-8 (sc-81657), and caspace-9 (sc-56073) were purchased from Santa Cruz Biotechnology Inc., but Bcl2 (ab38629) and poly (ADP-ribose) polymerase (PARP) (ab4830) were purchased from Abcam plc (Cambridge, UK). The membranes were then incubated for 1 hour at room temperature with alkaline phosphatase conjugated goat anti-mouse or goat anti-rabbit secondary antibodies in a ratio of 1:5,000 and then washed twice with TBST for 10 minutes three times on an orbital shaker. Then, the blots were developed using the BCIP/NBT (Santa Cruz Biotechnology Inc.) for sensitive colorimetric detection to quantify the target protein band.

Determination of the intracellular reactive oxygen species (ROS) level

ROS was determined with 2′,7′-dichlorofluorescin diacetate (DCFH-DA).[30–32] Concisely, 10 mM DCFH-DA stock solution (in methanol) was diluted 500-fold in Hank's Balanced Salt Solution with no serum or further additives to yield a 20 µM working solution. After exposure to AM for 24 hours the cells in the 96-well black plate were rinsed two times with Hank's Balanced Salt Solution before incubating in a 100 µL working solution of DCFH-DA at 37°C for 30 minutes. Using a fluorescence microplate reader, Tecan Infinite®200 Pro, the result was taken in emission at 485-nm excitation and 520-nm emission.

DNA content and cell cycle phase distribution

MCF-7 cells at a concentration of 1×10^5 cells/mL were seeded into a 25 mL flask containing RPMI 1640 augmented with 10% FBS and dosed with AM 5, 10, and 20 µg/mL. After incubation for 24 hours, the cells were collected, centrifuged to remove the old medium, and washed two times using warm PBS, then the pellet was fixed with 90% cool ethanol (kept at −20°C for 1 day before use) and kept at 4°C overnight. After incubation, the cells were spun down for 5 minutes at 1,800 rpm, the ethanol was removed and the pellets were washed with PBS to clear ethanol from the fixed cells. An amount of 600 µL warmed PBS was added and mixed gently. Then, 25 µL RNase A in a concentration of 10 µg/mL and 50 µL of PI at a concentration 1 µg/mL were decanted into the pellet and preserved in a dark place for 30 minutes. The DNA content of the cells was then examined using a FACS Canto II Becton-Dickinson Flow cytometer by studying at least 10,000 cells per sample. The percentage of cells in the G_1, S, and G_2 phases was investigated using Diva software (BD Biosciences, San Jose, CA, USA).

Immunofluorescence of NF-κB activity

HCS was utilized to assess the inhibitory effects of AM on tumor necrosis factor alpha (TNF-α)-induced NF-κB activation, ie, nuclear translocation of NF-κB. The experiments were conducted according to the company's instructions for the NF-κB activation kit (Thermo Fisher Scientific). An ArrayScan reader was utilized to measure the variance between the strength of the nuclear and cytoplasmic NF-κB-associated fluorescence, and reported as a translocation parameter.

Human apoptosis proteome profiler array

To examine the pathways through which AM prompts apoptosis, we determined the apoptosis-related proteins utilizing the Proteome Profiler Array (RayBio® Human Apoptosis Antibody Array Kit, Raybiotech, Norcross, GA, USA), in accordance with the manufacturer's instructions. In short, the cells were dosed with 20 µg/mL AM. Three hundred µg proteins from each sample were incubated overnight with the human apoptosis array. The data from the apoptosis array were measured by scanning the membrane using a Biospectrum AC ChemiHR 40 (UVP, LLC, Upland, CA, USA) and examination of the file of the array image was conducted using image analysis software in accordance with the instructions of the company.

Mammary tumor implantation

Rat LA7 mammary adenocarcinoma cells at around 75%–85% confluence were trypsinized, washed once in Dulbecco's Modified Eagle's Medium (supplemented with 5% FBS), spun down, and suspended in the same medium. A total of two million cells in a volume of 100 µL were injected into the mammary fat pads of 20 female Sprague-Dawley rats.

Experimental design and treatment of implanted animals

Ten days after implantation of LA7 mammary carcinoma, the animals were randomly separated into six groups (n=5 per group): normal control; mammary tumor control (LA7-induced non-treated); low dose (treated with 30 mg/kg/day of AM dissolved in Tween 20); high dose (treated with 60 mg/kg/day of AM dissolved in Tween 20); tamoxifen (treated subcutaneously with 10 mg/kg/day of tamoxifen dissolved in Tween 20); and AM (normal rats treated with 60 mg/kg/day of AM dissolved in Tween 20). All treatments by AM were selected based on the toxicological report by

Ibrahim et al,[30] and given to the animals orally twice a week for 28 days using a gastric tube. At the end of treatment, the rats were euthanized and the entire tumor was removed, sectioned, and fixed in 10% paraformaldehyde. All experimental procedures performed on animals were done according to regulations set by the Institutional Animal Ethical Committee (FAR/20/04/2013/MYID), Faculty of Medicine, University of Malaya.

Evaluation of effect of AM on tumor size

The total tumor volume (mm^3) was quantified by multiplication of the slice sections and by summing the segmented areas.

Statistical analysis

The results were reported as the mean ± standard deviation for at least three analyses for each sample. The normality and homogeneity of variance assumptions were checked, and statistical analysis was performed according to the SPSS 16.0 package (SPSS Inc., Chicago, IL, USA) and GraphPad prism 5.0 (GraphPad Software, Inc., La Jolla, CA, USA). Analysis of variance was performed using the ANOVA procedure.

Results

AM inhibits the growth of MCF-7 cells

The cytotoxic effects of AM on the MCF-7 cells were ascertained by means of MTT assay. As shown in Table 1, AM inhibited the growth of MCF-7 cells and significant inhibition was exhibited at 10.26±0.25 µg/mL after 24 hours. Tamoxifen, which was used as standared control, showed an IC_{50} of 2.35 µg/mL. Meanwhile, AM did not exhibit any cytotoxicity toward the normal breast cell line MCF-10A with IC_{50} >30 µg/mL.

AO-PI double staining cell morphological analysis

To determine the viable cells, as well as those in early apoptosis, late apoptosis and secondary necrosis, the cells were counted using a fluorescence microscope. A total of 200 cells were counted arbitrarily and differentially, along with the negative control, which was untreated. Early apoptosis was detected using AO within the fragmented DNA with a bright green fluorescence. In addition, the green nuclear structure of the control cells was shown to be intact (Figure 1B). Following treatment with 5 µg/mL AM, moderate apoptosis was observed by blebbing and nuclear chromatin condensation (Figure 1C). In addition, in the later phases of apoptosis, alterations, including a reddish-orange color due to the binding of AO to the denatured DNA, were noted after AM 10 and 20 µg/mL of treatment (Figure 1D and E). The results indicated that the AM produced morphological features that are linked to apoptosis in a concentration-dependent manner. A statistically significant ($P<0.05$) difference was noted in the cell population through the differential recording of treated cells (200-cell population) (Figure 1F).

Table 1 IC_{50} concentrations of AM and tamoxifen

Cell line	IC_{50} ± SD (µg/mL)	
	AM	Tamoxifen
MCF-7	10.26±0.25	2.35±0.35
MCF-10A	>30	18.9±0.12

Abbreviations: IC_{50}, half-maximal inhibitory concentration; AM, α-Mangostin; SD, standard deviation.

Effect of AM on the ratio of apoptotic cells by AV-FITC staining

Flow cytometric analysis, with AV/PI double staining, was used to confirm the induced apoptotic effect of AM by determining the percentage of apoptotic cells. The AV^+/PI^- staining signifies the early apoptotic cells because of the strength of the affinity between AV-FITC and phosphatidylserine that transported from the inner leaflet to the outer surface of the plasma membrane in early apoptosis. In contrast, AV^-/PI^+ staining signifies the necrotic cells, as PI, which cannot penetrate an undamaged cell membrane, passes through the affected membrane of the dead cells or late apoptotic cells, and binds to the nucleic acid. In addition, viable cells are marked by AV^-/PI^-, and AV^+/PI^+ staining, which is symbolic of the late apoptotic cells. The characteristic dot plots of the flow cytometric assessment of apoptosis indicated that according to the evaluation of the untreated cells (control) and treated cells (with 5, 10, and 20 µg/mL AM), the percentages in early apoptosis and late apoptosis increased respectively (Figure 2). Moreover, the AM treatment clearly resulted in slightly fewer viable cells at 5 and 10 µg/mL. In addition, the results indicated that the anti-proliferative effect of AM in respect of MCF-7 cells was instigated by triggering cell apoptosis.

AM-induced apoptosis in MCF-7 cells

To verify the occurrence of apoptosis, we inspected the alterations in the nuclear morphology of the MCF-7 cells by determining the nuclear condensation and

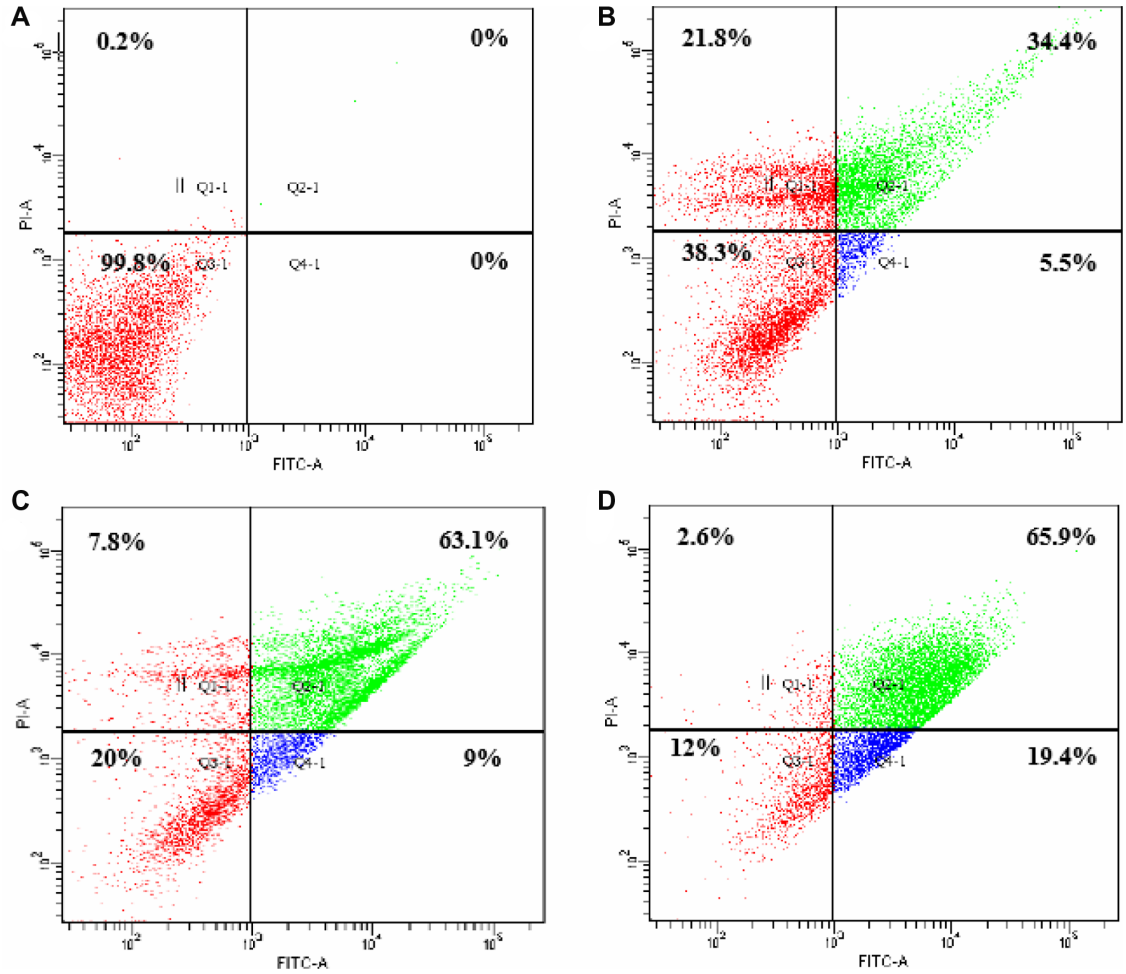

Figure 2 The effect of AM on early apoptosis of MCF-7 cells.
Notes: MCF-7 cells were exposed to different concentrations of AM and incubated for 24 hours at 37°C in a CO_2 incubator. After staining with FITC-conjugated Annexin V and PI, cells were analyzed by flow cytometry. Control cells received no drug treatments. The early apoptotic events (AV^+/PI^-) are shown in lower right quadrant (Q4-1) of each panel. Quadrant (Q2-1) represents AV^+/PI^+ late stage of apoptosis/dead cells. (**A**) The MCF-7 control (n=3). (**A**–**D**) The effects of 0, 5, 10, and 20 μg/mL exposures (respectively) of MCF-7 cells to AM.
Abbreviations: AM, α-Mangostin; FITC, fluorescein isothiocyanate; AV, Annexin V; PI, propidium iodide.

fragmentation hallmark for apoptosis (Figure 3A). Hoechst 33342 staining indicated that some of the cells exhibited nuclear condensation with 20 μg/mL AM treatment. The intensity of the nucleus that directly relates to the apoptotic chromatin changes, such as blebbing, fragmentation, and condensation, are quantified in Figure 3B. A simultaneous increase in the cells' permeability was also observed (Figure 3C).

AM-induced MMP disruption and release of cytochrome c

In the apoptosis, MMP is often disturbed by the forming of permeability transition pores or the insertion of pro-apoptotic proteins like Bax or BH3 interacting domain death agonist (Bid) in the membrane of mitochondria. Hence, we studied the effect of AM on the MMP of MCF-7 cells with the use of a mitochondria-specific voltage-dependent dye. As displayed in Figure 3D, the MMP in the cells treated with AM ($P<0.05$) showed a considerable reduction. In addition to that, a considerable decrease in the intensity of fluorescence (Figure 3A), which reflected the breakdown of MMP, AM also activated a major translocation of cytochrome c from the mitochondria into the cytosol. At 20 μg/mL, AM activated three times the amount of cytochrome c released in MCF-7 cells compared to the control ($P<0.05$) (Figure 3E). Moreover, since the release of cytochrome c from the mitochondria triggers the activation of pro-caspace 9, we measured the immunoblotting of cytosol cytochrome c. In a concentration-dependent manner, AM significantly increased the level of cytosol cytochrome c in MCF-7 cells compared to the control ($P<0.05$) (Figure 8D).

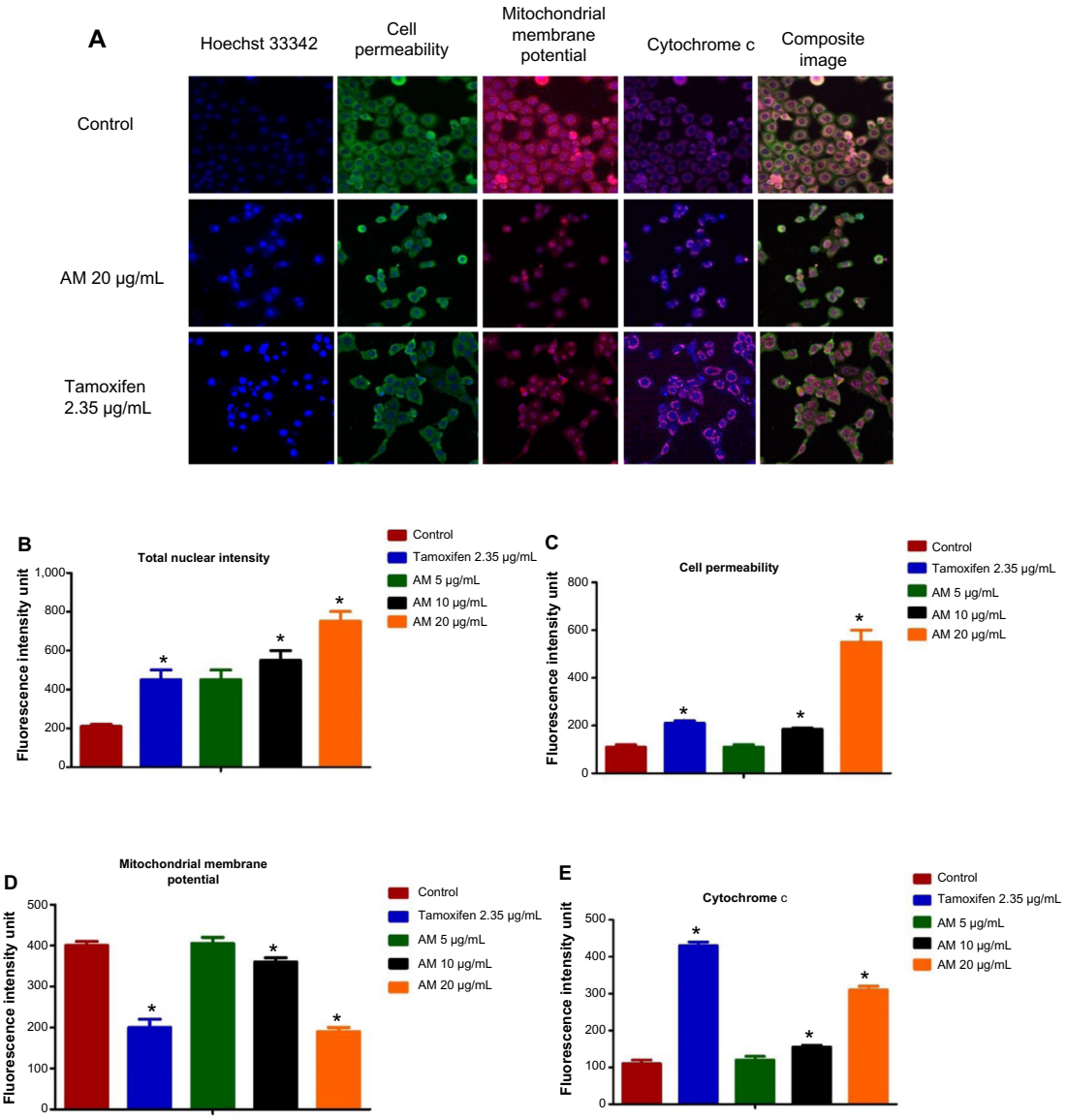

Figure 3 Effect of AM on MMP, permeability and cytochrome c release.
Notes: (**A**) Representative images of MCF-7 cells treated with medium alone, 5 µg/mL, 10 µg/mL, and 20 µg/mL of AM, and stained with Hoechst for nuclear, cell permeability dye, MMP, and cytochrome c. The images from each row were obtained from the same field of each sample (magnification 20×). (**B**–**E**) Average fluorescence intensities of Hoechst 33342, cell permeability dye, MMP, and cytochrome c in MCF-7 cells treated with AM or standard drug tamoxifen. Data were mean ± SD of fluorescence intensity readings measured from different photos taken (*$P<0.05$).
Abbreviations: AM, α-Mangostin; SD, standard deviation; MMP, mitochondrial membrane potential.

AM regulates the expression of Bcl-2 and Bax protein

The expression of pro-apoptotic proteins, such as Bax, is an early incident that sensitizes cells to undergo apoptosis. Compared with the controls, MCF-7 cells that were treated with AM displayed a considerable escalation in fluorescence intensity (Figure 4A) when stained using a specific Bax antibody. This outcome indicated that the expression of Bax is upregulated in MCF-7 cells after dosing with 20 µg/mL AM. Nevertheless, the anti-apoptotic, Bcl-2 levels were minimal during the period of treatment (Figure 3A). Figure 3B shows that both up and downregulation of Bax and Bcl-2 were statistically significant ($P<0.05$) in concentration dependent manner. To confirm the immunofluorescence result, the expression of Bax and Bcl-2 in the MCF-7 cells treated with AM were determined using Western blot analysis. AM treatment resulted in an upregulation of Bax and a downregulation of Bcl-2 in concentration dependent manner (Figure 4C), which resulted in an increase in the ratio of Bax to Bcl-2, therefore favoring apoptosis (Figure 4D).

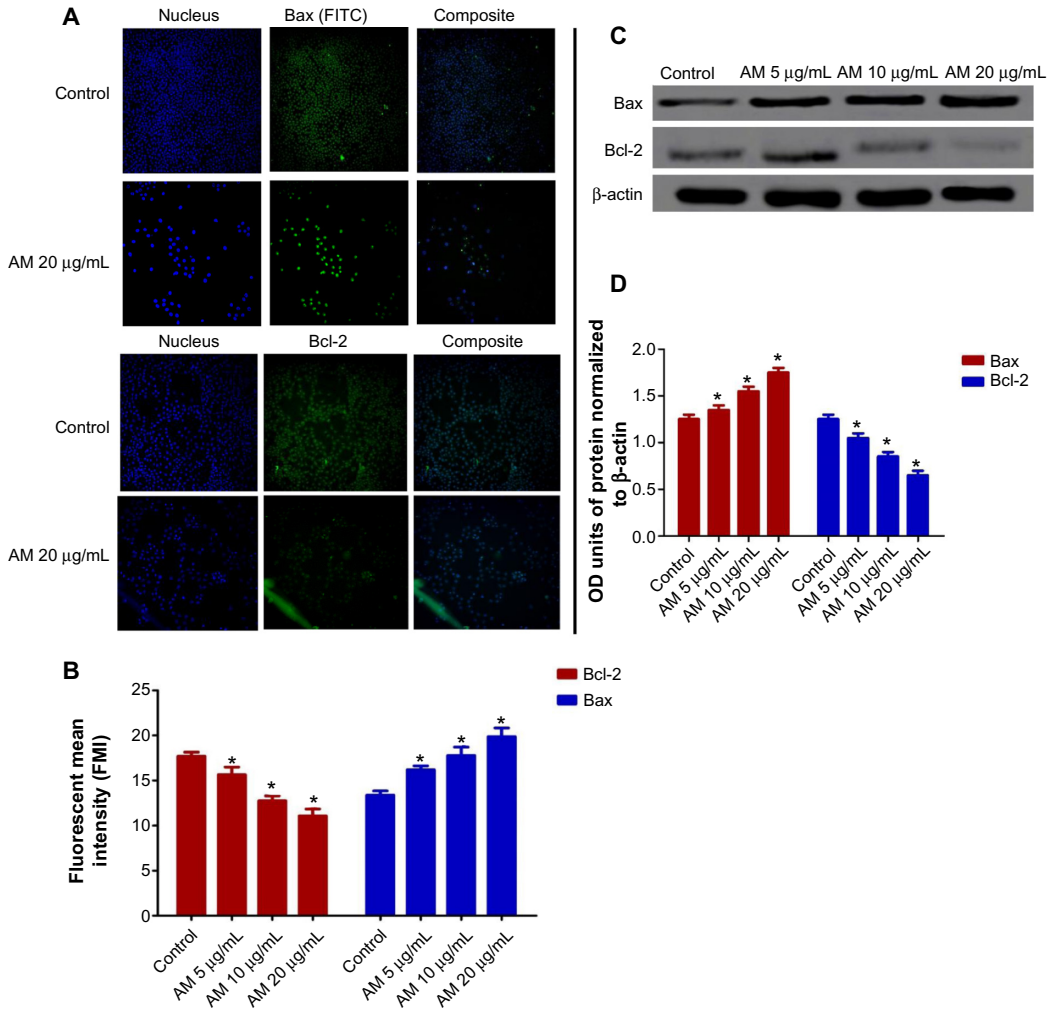

Figure 4 AM changes the regulation of Bax/Bcl-2 expression.
Notes: MCF-7 cells were treated with 5 μg/mL, 10 μg/mL, and 20 μg/mL of AM. (**A**) Cells were stained with Hoechst 33342 for nucleus and FITC flurochrome-conjugated secondary antibody for Bax and Bcl-2 expression respectively (magnification 20×). (**B**) Fluorescence intensity of FITC in cells treated with designated concentration of AM. Data are shown as mean ± SD. Significant differences (*$P<0.05$) between AM-treated and untreated control cells. (**C**) Western blot analysis of Bax and Bcl-2 after treatment with 5 μg/mL, 10 μg/mL, and 20 μg/mL of AM. (**D**) The blot densities are expressed as folds of control. Data are mean ± SD (n=3). *$P<0.05$ versus control.
Abbreviations: Bax, Bcl-2-associated X protein; Bcl-2, B-cell lymphoma 2; AM, α-Mangostin; FITC, fluorescein isothiocyanate; SD, standard deviation; OD, optical density.

Effect of AM treatment on caspace-3/7, -8, and 9

All the caspace enzymes being examined were shown to be induced by the treatment, and were concentration-dependent. A high level of caspace 3/7 was found in the greatest treatment concentration (20 μg/mL) with a significant variance from the control ($P<0.05$) for both types of cell. Although significant levels of caspace-8 and caspace-9 were found in both, the triggering of caspace was not found to be significantly prompted for caspace 3/7 at 5 and 10 μg/mL. Our results provide further validation of the activation of all three caspaces by AM in MCF-7 cells (Figure 5A). To confirm the immunofluorescence result, the cell extracts were obtained after treatments and processed for Western blot analysis. The changes in protein levels in the MCF-7 cells treated with different concentrations of AM were determined using Western blot analysis. In a concentration dependent manner, AM treatment resulted in partial cleavage of pro-caspace-7, -9, and -8 (Figure 5B), which indicated that AM could increase the cleavage maturation of caspace-7, -9, and -8 (Figure 5C).

Suppression of the PCNA and PARP protein expressions by AM

The expression of PCNA and PARP cleavage on MCF-7 cells with or without AM treatment was tested by Western

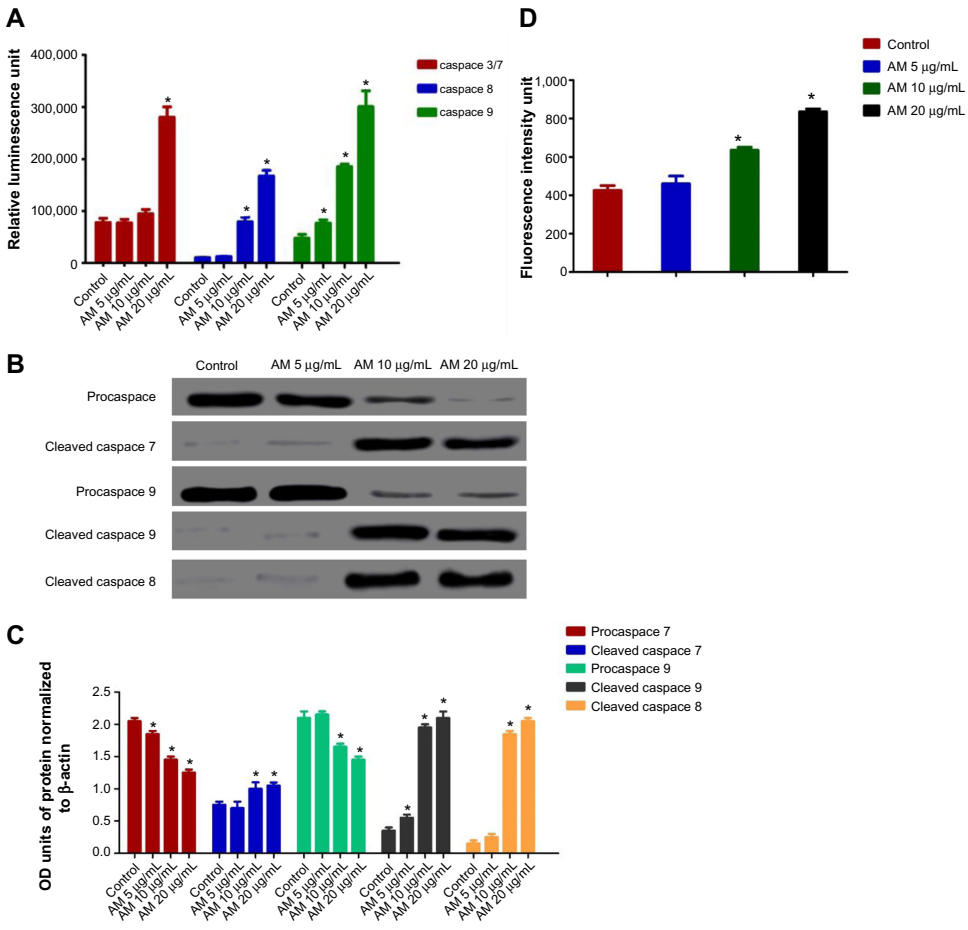

Figure 5 Effects of AM on MCF-7 cells' procaspaces, caspaces, cleaved caspaces, and ROS generation.
Notes: (**A**) Relative luminescence expression of caspaces in the MCF-7 cells treated with 5 µg/mL, 10 µg/mL, and 20 µg/mL of AM. (**B**) Western blot analysis of procaspaces and cleaved caspaces after treatment with 5 µg/mL, 10 µg/mL, and 20 µg/mL of AM. (**C**) The blot densities of procaspaces and cleaved caspaces are expressed as folds of control. Data are mean ± SD (n=3). *$P<0.05$ versus control. (**D**) Relative DCF-fluorescence intensity (ROS) after 5, 10, and 20 µg/mL of AM exposure at 24 hours. Values are mean ± SD from three independent experiments. Triplicates of each treatment group were used in each independent experiment. The statistical significance is expressed as *$P<0.05$.
Abbreviations: AM, α-Mangostin; SD, standard deviation; DCF, 2',7'-dichlorofluorescin; ROS, reactive oxygen species; OD, optical density.

blot analysis. As shown in Figure 8D and E, after treatment with 5, 10, and 20 µg/mL of AM, the level of PCNA protein decreased significantly. Since PARP cleavage results in a cleaved product of 89 kDa, we have observed the reduction in the PARP (116 kDa) and concomitant presence of a cleaved product in a dose-dependent manner (Figure 8D and E).

AM-induced cell death includes increased ROS formation

The production of ROS was generally linked to the MMP disturbance and cell apoptosis. To determine the relation, we inspected the levels of ROS in MCF-7 cells treated with AM. ROS was observed by the oxidation-sensitive fluorescent dye DCFH-DA. The escalation of dose-dependence in DCF fluorescence was observed in the treated cells. In addition, a considerable and immediate formation of ROS, up to twice as high as observed in the control, was identified following the dosing of cells with AM at 10 and 20 µg/mL (Figure 5D). This result indicated that this compound triggered the intracellular ROS development of MCF-7 cells.

Cell cycle analysis

We conducted this trial to determine the influence of AM on the DNA content of MCF-7 cells by the cell cycle phase distribution (G_0, G_1, S, G_2, and M) after treatment (Figure 6). The results indicated that AM halted the cell cycle progression in the G_0/G_1 phase ($P<0.05$). The results displayed in Figure 6E show that there is a significant G_0/G_1 phase arrest in a concentration-dependent manner in the MCF-7 cells, which accounts for 52.44%, 55.28%, and 68.75% of cells following treatment with 5, 10, and 20 µg/mL, respectively, for 24 hours ($P<0.05$). Meanwhile, the cells in both the S and G_2/M phases diminished with an increase in the treatment concentration.

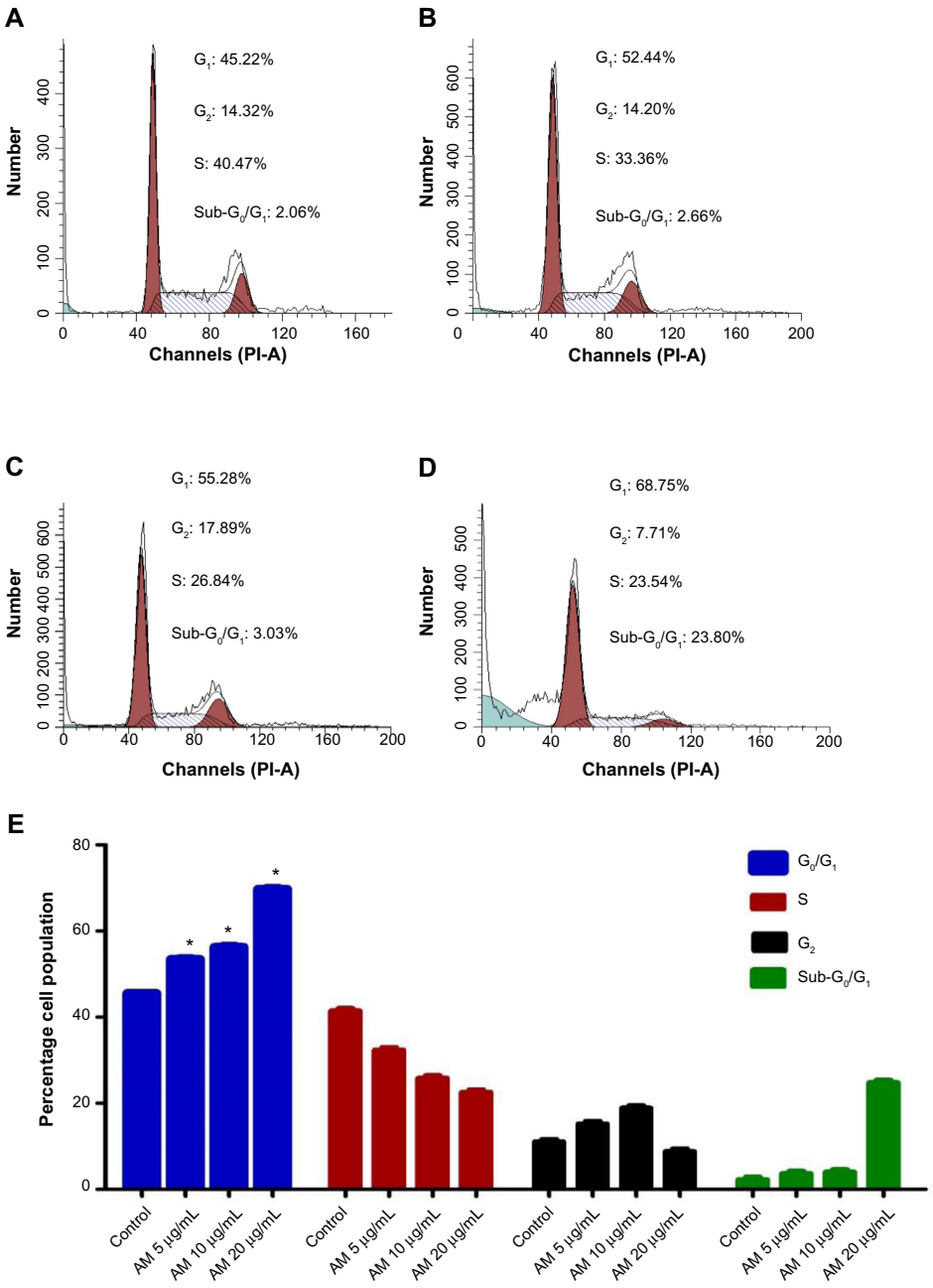

Figure 6 AM induced G_0/G_1 phase cell cycle arrest in MCF-7 cells.
Notes: Histograms for cell cycle from analysis of MCF-7 cells treated with AM at 5 (**B**), 10 (**C**), and 20 μg/mL (**D**), where (**A**) is control. Results are representative of one of three independent experiments. (**E**) Induction of G_0/G_1 phase arrest in the cell cycle progression of MCF-7 cells by AM. *Indicates a significant difference ($P<0.05$).
Abbreviation: AM, α-Mangostin.

Inhibition of TNF-α-induced NF-κB nuclear translocation by AM

The obstruction to apoptosis and cell proliferation was considered to be closely related to the activation of nuclear factor kappa-B (NF-κB). Hence, the role of AM in the suppression of activated NF-κB induced by the inflammatory cytokine, TNF-α, was examined using Alexa Fluor 488-conjugated anti-NF-κB antibody (Thermo Fisher Scientific, Waltham, MA, USA). Although a high NF-κB fluorescent intensity was observed in the cytoplasm in the control cells (medium alone) (Figure 7A), it was only faint in the nuclei, which suggests an absence of NF-κB activation in the control cells (medium alone). In addition, TNF-α alone considerably intensified the NF-κB fluorescent intensity in the nuclei. AM demonstrated a considerable inhibitory effect on the triggering of NF-κB (Figure 7B). In the cells treated with curcumin, a known inhibitor of NF-κB activation, a significant suppression of TNF-α-induced NF-κB nuclear translocation was observed,

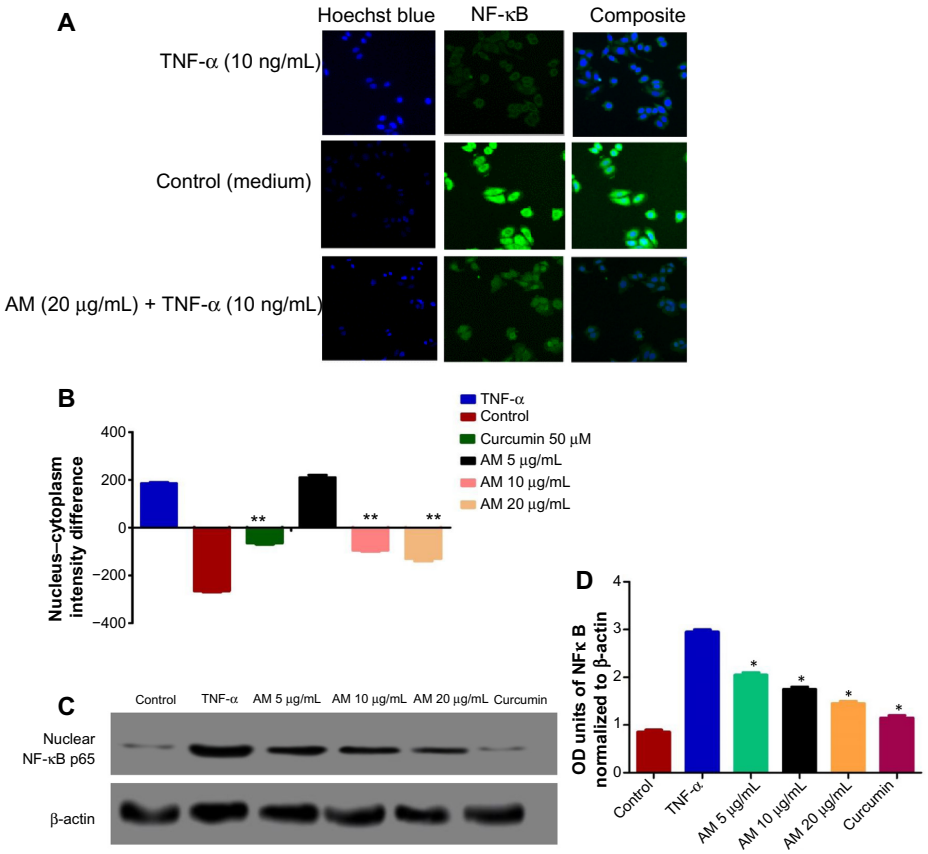

Figure 7 Photographs (**A**) and dose–response histogram for quantitative image analysis of intracellular targets (**B**) of stained MCF-7 cells that were treated with 20 μg/mL AM for 2 hours and then stimulated for 30 minutes with 10 ng/mL TNF-α (NF-κB activation). Triplicates of each treatment group were used in each independent experiment. The statistical significance is expressed as $^{**}P<0.01$. (**C**) Immunoblot analysis of nuclear NF-κB p65. (**D**) The blot densities of nuclear NFκB p65 are expressed as folds of control. Data are mean ± SD (n=3). $^{*}P<0.05$ versus control.

Abbreviations: AM, α-Mangostin; NF-κB, nuclear factor-kappa B; TNF-α, tumor necrosis factor alpha; ng, nanogram; SD, standard deviation; OD, optical density.

as evidenced by the low nuclear NF-κB-related fluorescence intensity (Figure 7B). In parallel, the morphological alterations of NF-κB translocation, as shown by the immunofluorescence staining (Figure 7A), indicated the inhibitory effect of AM on TNF-α-induced NF-κB translocation in a concentration-dependent manner with significant inhibition for the 20 μg/mL concentration of AM. To affirm the immunofluorescence result, we measured the immunoblotting of the nuclear content of NF-κB p65. As shown in Figure 7C and D, treatment with AM significantly decreased the escalation of this nuclear protein induced by positive control (TNF-α) in a dependent manner, particularly at 20 μg/mL of AM.

Human apoptosis protein array

Following AM exposure for 24 hours, the MCF-7 cells were lysed, and the apoptotic markers were screened using a protein array (Figures 8 and S1). In Figure 8C, the images show representative changes detected. All the major markers responsible for the apoptosis signaling pathway, including Bax, Bcl-2, Bim, cytochrome c, caspace-3/7 and -8 were expressed in the two models. A significant chaperone Hsp70, which played a part in the apoptosis was also downregulated, while the cell proliferation repressor protein p27, as well as X-linked inhibitor of apoptosis protein (XIAP) were also induced in this in vitro model. To confirm the protein array result, the expression of Hsp70 in the MCF-7 cells treated with AM was determined using Western blot analysis. AM treatment resulted in a downregulation of this protein in a concentration dependent manner (Figure 8D and E).

AM reduced tumor size in vivo

Table 2 presents the volume and the reduction of tumor percentage (%) of control and experimental animals. The tumor growth was measured using a caliper. The tumors in the mammary tumor control group grew rapidly, reaching an average volume of 1,737±563 mm^3 by day 28. Meanwhile, groups treated with AM 30 mg/kg and 60 mg/kg showed a significant ($P<0.05$) reduction in their tumor volume when compared with the mammary tumor

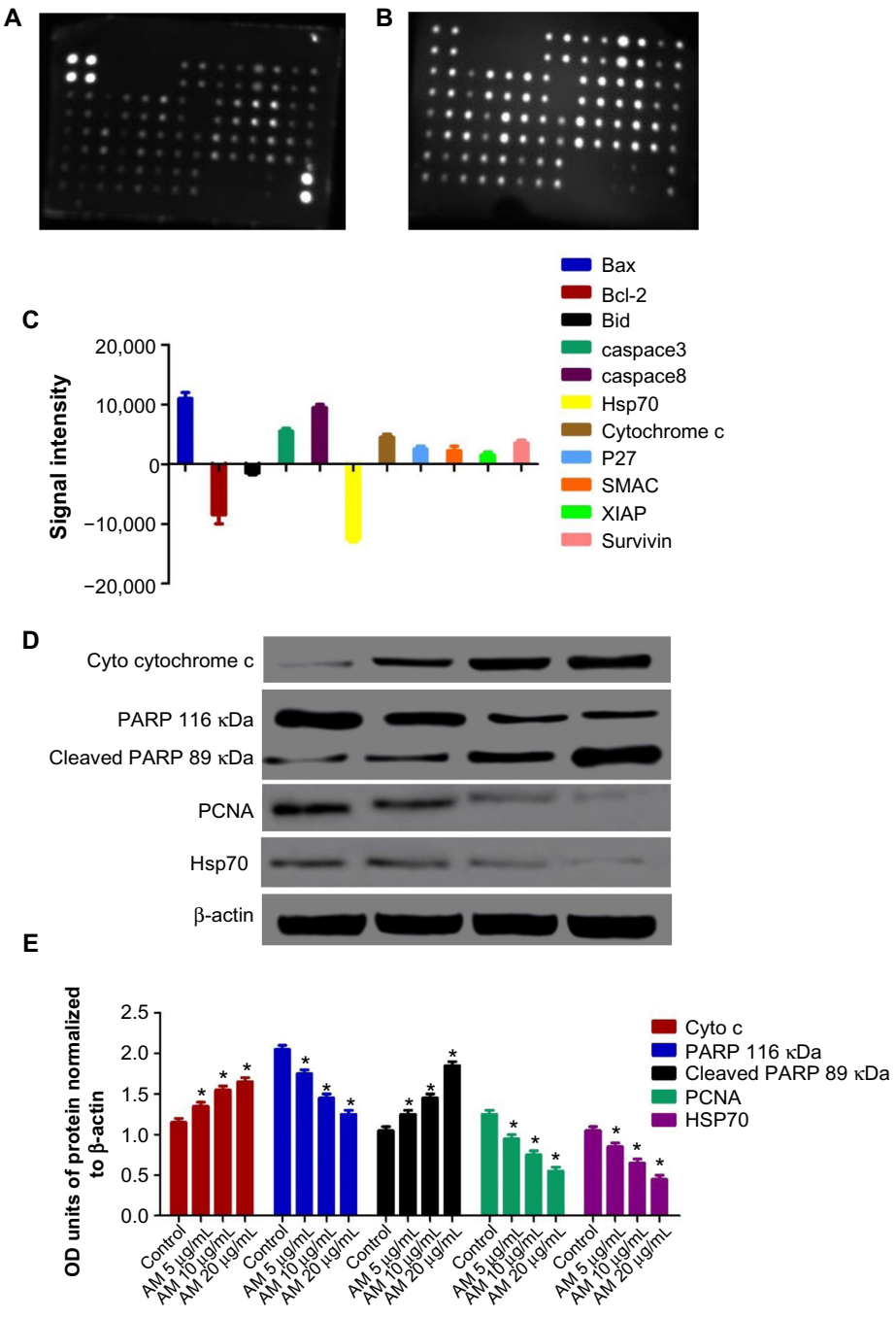

Figure 8 MCF-7 cells were lysed and protein arrays were performed.

Notes: Cells were treated with 20 μg/mL AM and the whole cell protein was extracted. Equal amounts of (300 μg) of protein from each sample were used for the assay. Representative images of the apoptotic protein array are shown for the control (**A**) and treatment (**B**). Quantitative analysis in the arrays showed differences in the apoptotic markers (**C**). Immunoblot analysis of cytosolic cytochrome c, cleaved PARP, PCNA, and Hsp70 (**D**). The blot densities of cytosolic cytochrome c, PARP, cleaved PARP, PCNA, and Hsp70 are expressed as folds of control (**E**). Data are mean ± SD (n=3). *$P<0.05$ versus control.

Abbreviations: AM, α-Mangostin; Bax, Bcl-2-associated X protein; Bcl-2, B-cell lymphoma 2; Bid, BH3 interacting domain death agonist; Hsp70, heat shock protein 70; SMAC, second mitochondria-derived activator of caspace; XIAP, X-linked inhibitor of apoptosis protein; P27, cyclin-dependent kinase inhibitor 1B; PARP, poly ADP-ribose polymerase; SD, standard deviation; PCNA, proliferating cell nuclear antigen; OD, optical density.

control group. The AM 60 mg/kg treatment also resulted in greater reduction (79.2%) in tumor volume than the AM 30 mg/kg treatment (74.1%), whilst tamoxifen (10 mg/kg) treated groups reduced the mammary tumor by an average of 83.6% (Figure 9).

Discussion

The role of apoptosis, which is a highly regulated process of programmed cell destruction, is crucial in many functions, ranging from fetal development to adult tissue homeostasis.[31] Tumors are attributed to uncontrolled

Table 2 Effect of treatment with AM 30 mg/kg, AM 60 mg/kg and tamoxifen on tumor volume (mm^3) in experimental breast cancer in rats

Treatment groups	Tumor volume (mm^3)	Reduction of tumor percentage (%)
Normal control	–	–
Mammary tumor control	1,773±563	–
AM 30 mg/kg LD	460±33.5*	74.1%*
AM 60 mg/kg HD	372±24.6*	79.2%*
Tamoxifen 10 mg/kg	290±21*	83.6%*
AM 60 mg/kg	–	–

Notes: Each value represents mean ± SD of given number of animals (n=5). The statistical significance is expressed as *$P<0.05$.
Abbreviations: AM, α-Mangostin; LD, low dose; HD, high dose; SD, standard deviation.

proliferation as well as reduced apoptosis. One critical method by which cytotoxic drugs destroy cancer cells is the activation of apoptotic pathways.[32] Herbal medicines have been a major source from which numerous apoptosis-inducing agents are derived,[33] and, according to several reports, many of these naturally occurring compounds may contribute partially to human cancer prevention or therapy.[34] These studies showed that bioactive compounds elicit apoptosis in cancer cells.[35] Renewed interest in the application of oriental medicine for cancer treatment, along with auspicious clinical results, has led to much emphasis being placed on medicinal plants. Nevertheless, the chemical components as well as definite mechanisms of many herbal medicines remain obscure.

In this regard, *C. arborescens* is one of the well-known plants used in Asian countries for preventing and treating different kinds of ailments.[14] AM, as a natural compound, is a major prenylated xanthone isolated from this plant. Therefore, the present study elucidated the mechanism of apoptosis provoked by AM toward MCF-7 cells. According to Shier,[36] compounds that demonstrate an IC_{50} value of more than 30 µg/mL are considered as not potentially cytotoxic, while compounds with an IC_{50} value of less than 5.0 µg/mL are considered very active. These findings show that AM acts differently on normal cells compared to cancer cells that are more cytotoxic toward mammary gland cancer cells than normal cells. Since we found that the cytotoxicity produced by AM is within a potential limit, we used AO and PI fluorescent dyes to observe the different stages of apoptosis, beginning from the condensation of the chromatin up to the formation of apoptotic bodies, with AM treatment. Although the morphological features were clearly noticed, the assay of AV was conducted in an attempt to quantify the cells of the apoptotic population. The present study established that AM treatment can induce cell death in MCF-7 cells through apoptosis. In addition, the results showed a significant dose-dependent increase occurring in the early stage of apoptosis.

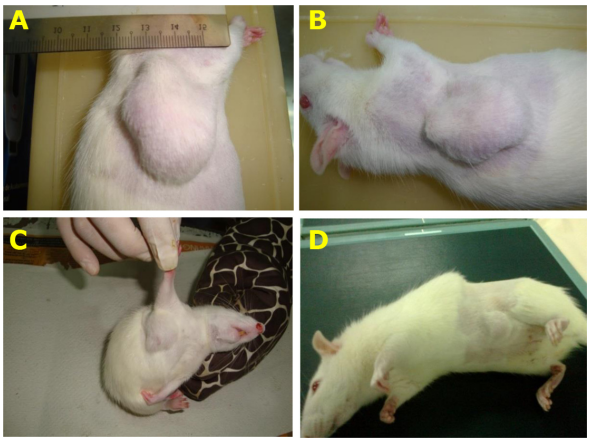

Figure 9 Therapeutic effect of AM treatment on LA7-induced mammary tumors in rats (4 weeks).
Notes: Reduction of tumor size of rats in treated groups: low dose 30 mg/kg AM (**B**), high dose 60 mg/kg AM (**C**), and tamoxifen 10 mg/kg (**D**) compared to the mammary tumor control (**A**).
Abbreviation: AM, α-Mangostin.

Although both extrinsic and intrinsic pathways are involved in apoptosis, the sensitivity of the intrinsic pathways causes tumors to occur more frequently through this route.[37] Mitochondria are the main cellular components for the intrinsic means of apoptosis due to their ability to directly initiate the apoptotic cellular program. The primary involvement of the mitochondria is in the cell's redox status, although they can also execute multiple cellular functions, including energy production, as well as cell proliferation and death.[38,39] The permeabilization of the outer membrane and alteration of the mitochondrial transmembrane potential ($\Delta\psi m$) by the mitochondria initiating the apoptotic cascade, releases soluble pro-apoptotic proteins including cytochrome c, which, ultimately, leads to the activation of caspaces 9 and 3.[37] It is essential that the potential of the mitochondria membrane is decreased for this process to begin. The effect of AM on the mitochondria, which causes less MMP was revealed by the fluorescence-based high content screening analysis. Concurrently, the release of cytochrome c also increased. There is much evidence that suggests that there is a role of oxidative stress in the apoptosis and related mitochondrial changes.[40] In order to check the involvement of ROS, we measured the ROS level upon AM treatment toward MCF-7. The results clearly underline this significant relation ($P<0.05$). There was elevated (3-fold) intracellular ROS with AM treatment (20 µg/mL) on MCF-7 cells and this could be due to the free radical generation during the cytotoxicity.

Concurrently, a number of Bcl-2 family members, including Bcl-2 and Bax, are known to have the ability to control apoptosis.[41] In ascertaining the vulnerability of cells toward death, it is crucial for a balance to exist between anti-apoptotic and pro-apoptotic Bcl-2 family members.[42] It has been shown in previous reports that susceptibility to mitochondria mediated apoptosis can be caused by the upregulation of Bax and downregulation of Bcl-2.[43,44] Thus, we examined the effect of AM on the expression of proteins that belong to this family. Bcl-2 is a cytoplasmic protein that has a significant part in inhibiting apoptosis that is caused by factors, such as chemotherapeutic agents, irradiation, as well as the withdrawal of growth factors.[45,46] The immunofluorescence results in this research demonstrated the Bcl-2 downregulation in MCF-7 cells after treatment with 20 µg/mL AM. This occurrence likely explains the apoptotic effects of AM on MCF-7 cells. The exertion of these effects on the expression of Bcl-2 may also be connected to the production of mitochondrial apoptotic factors, which, eventually, lead to apoptosis.[47] Our findings regarding AM support previous findings that showed that the induction of apoptosis seems to be modulated by the levels of Bcl-2 and Bax in the head and neck squamous carcinoma cell line (HNSCC), human Caucasian colon adenocarcinoma cell line (COLO 205), undifferentiated human colon carcinoma cell line (MIP-101), and human colon epithelial adenocarcinoma cell line (SW 620).[21,48]

Subsequently, with MMP disruption and the release of cytochrome c, AM treatment of MCF-7 cells triggered the activation of caspaces 3/7, 8, and 9. In fact, the stimulation of caspaces 9 and 8 happened with a minimum concentration of AM, while caspace 3/7 activation only took place at a maximum treatment concentration. caspace 9 is located in the intermembrane space of the mitochondria. It is discharged in a Bcl-2-inhibitable manner following the induction of permeability transition, whereas, in cells, the release is upon the induction of apoptosis.[49] The caspace 9 that has been released then activates the post-mitochondrial caspaces, which include caspaces 3 and 7; the disassembly of the cell takes place in what is termed the execution phase of apoptosis.[50] caspace 8 is closely implicated in apoptosis signaling via the extrinsic pathway, albeit it is found in the upstream and downstream of the mitochondria.[49,51] Moreover, the engagement of caspace 8 in mitochondrial pathways through the cleavage of the Bcl-2 family member Bid to tBid has been shown on numerous occasions.[52] Our results regarding AM are well correlated with a previous study on AM against BJMC3879 metastatic murine mammary adenocarcinoma cells that showed the activation of caspaces 3, 9, and 8.[53]

PARP can detect DNA damage due to its sensitivity. This enzyme is strongly triggered by DNA strand breaks and has primary functions in processes, such as DNA repair and the maintenance of genome stability. In addition, it also performs a crucial role in the induction of cell death initiated by a variety of stimuli.[54] The proteolytic degradation of PARP that takes place at the beginning of apoptosis is caused by the activated caspace 3.[55] As demonstrated by the immunoblot analysis, AM treatment significantly reduced PARP. Based on the results, it was shown that the stimulation of caspaces-9 and -3 is induced by the released cytochrome c, which, in turn, cleaves 116 kDa PARP into 85 kDa fragments in MCF-7 treated cells. PARP plays a crucial role in DNA repair and interacts with many DNA replication/repair factors, including the PCNA, a protein involved in many DNA transactions.[56] Our next aim was to detect the response of AM toward this interaction. The anti-proliferative efficacy of AM has been established as it was found to decrease the immunoblotting expression of this proliferative marker in MCF-7 cells.

The mode of apoptosis caused by numerous natural compounds is closely related to cell cycle arrest.[57–59] It has been established that cell cycle control is a significant event in safe-guarding precise cellular division. Many carcinogenic processes are reported to cause the abnormalities of cell cycle regulators. For this reason, it is reasonable to target and alter the cell cycle regulators in cancer cells for the purpose of chemoprevention and treatment.[60–62] Following dosage with various concentrations of AM, the examination of the cell cycle of MCF-7 cells exhibited a higher number of cells in the G_0/G_1 phase. On the other hand, the amount of cells in the S and G_2/M phase was reduced in comparison with the untreated cells (Figure 6). These results indicate the ability of AM in inhibiting cellular proliferation via G_0/G_1 phase arrest. This corroborates a previous study concerning the effect of AM against BJMC3879 cells, which demonstrated the inhibition of cellular proliferation via G_0/G_1 phase arrest.[53]

The nuclear factor kappa-light-chain-enhancer of activated B cells, also known as NF-κB, is a protein complex that plays a role in regulating DNA transcription. In addition, it has also been considered as an apoptosis inhibitor.[63,64] Thus, repression of the NF-κB activity can induce apoptosis. In this study, we have demonstrated that AM can prevent the TNF-α-induced NF-κB translocation of the cytoplasm to the nucleus of the MCF-7 cells, suggesting the participation of an NF-κB inhibition mechanism in apoptosis.

Apoptosis involves a large number of proteins.[65,66] To determine the role of the central apoptosis-related proteins, a protein array analysis was conducted. In this study, various proteins in the extrinsic and intrinsic pathways were examined. These proteins include those that are known to cause apoptosis, including Bax, caspace-3, cytochrome c, caspace-8, and second mitochondria-derived activator of caspace, as well as those that have been recognized as anti-apoptotic, including Bcl-2, XIAP, of which XIAP is a member of the inhibitors of apoptosis (IAP) family of proteins,[67] and second mitochondria-derived activator of caspace is a pro-apoptosis protein that acts together with IAP to reduce their inhibitory effects.[68,69] Together with the Bcl-2 family members, Hsps have also been deemed to be apoptosis inhibitors, due to their significant role in cell survival, through stopping the release of cytochrome c from mitochondria or by preventing the formation of apoptosome.[70] The protein array analysis showed a significant reduction in Hsp70 following treatment with AM. This finding is consistent with the findings from an earlier study[71,72] that indicated that apoptosis could be suppressed by an over-expression of Hsp70.[71,72] The results from the protein array displayed a characteristic profile of protein levels related to the mitochondrial apoptosis in MCF-7 cells treated with AM.

In the second part of this study, we also evaluated the effect of AM on tumor growth in Sprague-Dawley rats induced with LA7 cells to develop breast cancer for a duration of 28 days. The AM-treated groups (30 mg/kg and 60 mg/kg) showed significant tumor size reduction compared with the mammary cancer untreated group, indicating the potential chemotherapeutic value of AM in vivo. Our results regarding AM are well correlated with a previous study on AM against BJMC3879 metastatic murine mammary adenocarcinoma cells that showed the reduction of tumors after treatment with AM.[53]

According to the observations mentioned in this report, it can be concluded that AM has the ability to induce apoptosis in MCF-7 cells with cell death-transducing signals that regulate the MMP through a downregulation of Bcl2 and an upregulation of Bax, which, in turn, triggers the release of the cytochrome c from mitochondria to cytosol. The activation of caspace-9 is triggered once cytochrome c enters the cytosol, followed by the activation of the downstream executioner caspace-3/7. Subsequently, it cleaves specific substrates, making way for the occurrence of apoptotic changes. An increase of caspace-8 has shown the involvement of extrinsic pathways. This form of apoptosis was suggested to occur through both the extrinsic- and intrinsic-apoptosis pathways with regulation of NF-κB, Bax/Bcl-2, and Hsp70 protein modulation. In addition to that, ingestion of AM at (30 or 60 mg/kg) significantly reduced tumor size in an animal model of breast cancer.

Acknowledgments

This study was financially supported by the University of Malaya through the Postgraduate Research Fund (PPP) grant PG 141-2012B, University Malaya Research Grant RP001C-13BIO, and High Impact Research Grant UM-MOHE MC/625/1/HIR/MOHE//SC/09 from the Ministry of Higher Education Malaysia.

Disclosure

The authors declare that there are no conflicts of interest in this work.

References

1. Siegel R, Naishadham D, Jemal A. Cancer statistics, 2013. *CA Cancer J Clin*. 2013;63(1):11–30.
2. Hortobagyi GN, de la Garza Salazar J, Pritchard K, et al. The global breast cancer burden: variations in epidemiology and survival. *Clin Breast Cancer*. 2005;6(5):391–401.
3. Bray F, Ren J-S, Masuyer E, Ferlay J. Global estimates of cancer prevalence for 27 sites in the adult population in 2008. *Int J Cancer*. 2013;132(5):1133–1145.
4. Schottenfeld D, Beebe-Dimmer JL, Buffler PA, Omenn GS. Current perspective on the global and United States cancer burden attributable to lifestyle and environmental risk factors. *Annu Rev Public Health*. 2013;34:97–117.
5. Varghese JS, Smith PL, Folkerd E, et al. The heritability of mammographic breast density and circulating sex-hormone levels: two independent breast cancer risk factors. *Cancer Epidem Biomar*. 2012;21(12):2167–2175.
6. Charalambous C, Pitta CA, Constantinou AI. Equol enhances tamoxifen's anti-tumor activity by induction of caspase-mediated apoptosis in MCF-7 breast cancer cells. *BMC cancer*. 2013;13(1):238–244.
7. Yu X, Filardo EJ, Shaikh ZA. The membrane estrogen receptor GPR30 mediates cadmium-induced proliferation of breast cancer cells. *Toxicol Appl Pharmacol*. 2010;245(1):83–90.
8. Kuo JR, Wang CC, Huang SK, Wang SJ. Tamoxifen depresses glutamate release through inhibition of voltage-dependent Ca^{2+} entry and protein kinase Cα in rat cerebral cortex nerve terminals. *Neurochem Int*. 2012;60(2):105–114.
9. Pawar P, Ma L, Byon CH, et al. Molecular mechanisms of tamoxifen therapy for cholangiocarcinoma: role of calmodulin. *Clin Cancer Res*. 2009;15(4):1288–1296.
10. Abbasalipourkabir R, Salehzadeh A, Abdullah R. Antitumor activity of tamoxifen loaded solid lipid nanoparticles on induced mammary tumor gland in Sprague-Dawley rats. *African Journal of Biotechnology*. 2010;9(43):7337–7345.
11. Shukla Y, George J. Combinatorial strategies employing nutraceuticals for cancer development. *Ann N Y Acad Sci*. 2011;1229:162–175.
12. Cragg GM, Newman DJ. Natural products: A continuing source of novel drug leads. *Biochim Biophys Acta*. 2013;1830(6):3670–3695.
13. Tang J, Feng Y, Tsao S, Wang N, Curtain R, Wang Y. Berberine and Coptidis rhizoma as novel antineoplastic agents: a review of traditional use and biomedical investigations. *J Ethnopharmacol*. 2009;126(1):5–17.
14. José M, Kijjoa A, Gonzalez TG, et al. Xanthones from Cratoxylum maingayi. *Phytochemistry*. 1998;49(7):2159–2162.

15. Srithi K, Balslev H, Wangpakapattanawong P, Srisanga P, Trisonthi C. Medicinal plant knowledge and its erosion among the Mien (Yao) in northern Thailand. *J Ethnopharmacol*. 2009;123(2):335–342.
16. Obolskiy D, Pischel I, Siriwatanametanon N, Heinrich M. Garcinia mangostana L.: a phytochemical and pharmacological review. *Phytother Res*. 2009;23(8):1047–1065.
17. Pedraza-Chaverri J, Cárdenas-Rodríguez N, Orozco-Ibarra M, Pérez-Rojas JM. Medicinal properties of mangosteen (Garcinia mangostana). *Food Chem Toxicol*. 2008;46(10):3227–3239.
18. Pérez-Rojas JM, Cruz C, García-López P, et al. Renoprotection by α-mangostin is related to the attenuation in renal oxidative/nitrosative stress induced by cisplatin nephrotoxicity. *Free Radic Res*. 2009;43(11):1122–1132.
19. Saleem M. Lupeol, a novel anti-inflammatory and anti-cancer dietary triterpene. *Cancer Lett*. 2009;285(2):109–115.
20. Sampath PD, Kannan V. Mitigation of mitochondrial dysfunction and regulation of eNOS expression during experimental myocardial necrosis by alpha-mangostin, a xanthonic derivative from Garcinia mangostana. *Drug Chem Toxicol*. 2009;32(4):344–352.
21. Kaomongkolgit R, Chaisomboon N, Pavasant P. Apoptotic effect of alpha-mangostin on head and neck squamous carcinoma cells. *Arch Oral Biol*. 2011;56(5):483–490.
22. Wang JJ, Sanderson BJ, Zhang W. Significant anti-invasive activities of α-mangostin from the mangosteen pericarp on two human skin cancer cell lines. *Anticancer Res*. 2012;32(9):3805–3816.
23. Nelli GB, Kilari EK. Antidiabetic effect of α-mangostin and its protective role in sexual dysfunction of streptozotocin induced diabetic male rats. *Syst Biol Reprod Med*. 2013;45(2):1–10.
24. Koh JJ, Qiu S, Zou H, et al. Rapid bactericidal action of alpha-mangostin against MRSA as an outcome of membrane targeting. *Biochim Biophys Acta*. 2013;1828(2):834–844.
25. Kaomongkolgit R, Jamdee K, Chaisomboon N. Antifungal activity of alpha-mangostin against Candida albicans. *J Oral Sci*. 2009;51(3):401–406.
26. Ngawhirunpat T, Opanasopi P, Sukma M, Sittisombut C, Kat A, Adachi I. Antioxidant, free radical-scavenging activity and cytotoxicity of different solvent extracts and their phenolic constituents from the fruit hull of mangosteen (Garcinia mangostana). *Pharm Biol*. 2010;48(1):55–62.
27. Kumar RB, Shanmugapriya B, Thiyagesan K, Kumar SR, Xavier SM. A search for mosquito larvicidal compounds by blocking the sterol carrying protein, AeSCP-2, through computational screening and docking strategies. *Pharmacognosy Res*. 2010;2(4):247–253.
28. Devalaraja S, Jain S, Yadav H. Exotic fruits as therapeutic complements for diabetes, obesity and metabolic syndrome. *Food Res Int*. 2011;44(7):1856–1865.
29. Looi CY, Arya A, Cheah FK, et al. Induction of apoptosis in human breast cancer cells via caspase pathway by vernodalin isolated from Centratherum anthelminticum (L.) seeds. *PloS One*. 2013;8(2):e56643.
30. Ibrahim MY, Hashim NM, Mohan S, et al. α-Mangostin from *Cratoxylum arborescens*: an in vitro and in vivo toxicological evaluation. *Arabian J Chem*. Epub 2013.
31. Yang HS, Kim JY, Lee JH, et al. Celastrol isolated from Tripterygium regelii induces apoptosis through both caspase-dependent and -independent pathways in human breast cancer cells. *Food Chem Toxicol*. 2011;49(2):527–532.
32. Zhang X, Wei H, Liu Z, et al. A novel protoapigenone analog RY10-4 induces breast cancer MCF-7 cell death through autophagy via the Akt/mTOR pathway. *Toxicol Appl Pharmacol*. 2013;270(2):122–128.
33. Pacifico S, Gallicchio M, Lorenz P, et al. Apolar Laurus nobilis leaf extracts induce cytotoxicity and apoptosis towards three nervous system cell lines. *Food Chem Toxicol*. 2013;62(2):628–637.
34. Tanaka T. Role of apoptosis in the chemoprevention of cancer. *J Exp Clin Med*. 2013;5(3):89–91.
35. Pan M-H, Lai C-S, Wang H, Lo C-Y, Ho C-T, Li S. Black tea in chemoprevention of cancer and other human diseases. *Food Science and Human Wellness*. 2013;2(1):12–21.
36. Shier WT. Mammalian cell culture on $5 a day: a laboratory manual of low cost methods. *Los Banos, University of the Philippines*. 1991;64(8):9–16.
37. Constant Anatole P, Guru SK, Bathelemy N, et al. Ethyl acetate fraction of Garcina epunctata induces apoptosis in human promyelocytic cells (HL-60) through the ROS generation and G0/G1 cell cycle arrest: a bioassay-guided approach. *Environ Toxicol Pharmacol*. 2013;36(3):865–874.
38. Olguín-Martínez M, Hernández-Espinosa DR, Hernández-Muñoz R. α-Tocopherol administration blocks adaptive changes in cell NADH/NAD^+ redox state and mitochondrial function leading to inhibition of gastric mucosa cell proliferation in rats. *Free Radic Biol Med*. 2013;65(4):1090–1100.
39. Giorgi C, Romagnoli A, Pinton P, Rizzuto R. Ca^{2+} signaling, mitochondria and cell death. *Curr Mol Med*. 2008;8(2):119–130.
40. Ham Y-M, Yoon W-J, Park S-Y, et al. Quercitrin protects against oxidative stress-induced injury in lung fibroblast cells via up-regulation of Bcl-xL. *J Funct Foods*. 2012;4(1):253–262.
41. Czabotar PE, Lessene G, Strasser A, Adams JM. Control of apoptosis by the Bcl-2 protein family: implications for physiology and therapy. *Nat Rev Mol Cell Biol*. 2014;15(1):49–63.
42. Adams JM, Cory S. The Bcl-2 apoptotic switch in cancer development and therapy. *Oncogene*. 2007;26(9):1324–1337.
43. Lee JS, Jung W-K, Jeong MH, Yoon TR, Kim HK. Sanguinarine induces apoptosis of HT-29 human colon cancer cells via the regulation of Bax/Bcl-2 ratio and caspase-9-dependent pathway. *Int J Toxicol*. 2012;31(1):70–77.
44. Zhu AK, Zhou H, Xia JZ, et al. Ziyuglycoside II-induced apoptosis in human gastric carcinoma BGC-823 cells by regulating Bax/Bcl-2 expression and activating caspase-3 pathway. *Braz J Med Biol Res*. 2013;46(3):670–675.
45. Ferenc P, Solár P, Kleban J, Mikeš J, Fedoročko P. Down-regulation of Bcl-2 and Akt induced by combination of photoactivated hypericin and genistein in human breast cancer cells. *J Photochem Photobiol B*. 2010;98(1):25–34.
46. Zhang G-J, Kimijima I, Onda M, et al. Tamoxifen-induced apoptosis in breast cancer cells relates to down-regulation of bcl-2, but not bax and bcl-xL, without alteration of p53 protein levels. *Clin Cancer Res*. 1999;5(10):2971–2977.
47. Jin S, Zhang QY, Kang XM, Wang JX, Zhao WH. Daidzein induces MCF-7 breast cancer cell apoptosis via the mitochondrial pathway. *Ann Oncol*. 2010;21(2):263–268.
48. Watanapokasin R, Jarinthanan F, Nakamura Y, Sawasjirakij N, Jaratrungtawee A, Suksamrarn S. Effects of α-mangostin on apoptosis induction of human colon cancer. *World J Gastroenterol*. 2011;17(16):2086–2095.
49. Mohan S, Abdelwahab SI, Kamalidehghan B, et al. Involvement of NF-κB and Bcl2/Bax signaling pathways in the apoptosis of MCF7 cells induced by a xanthone compound Pyranocycloartobiloxanthone A. *Phytomedicine*. 2012;19(11):1007–1015.
50. Li Z, Jo J, Jia JM, et al. Caspase-3 activation via mitochondria is required for long-term depression and AMPA receptor internalization. *Cell*. 2010;141(5):859–871.
51. Jin Z, Li Y, Pitti R, et al. Cullin3-based polyubiquitination and p62-dependent aggregation of caspase-8 mediate extrinsic apoptosis signaling. *Cell*. 2009;137(4):721–735.
52. Gu Q, Wang JD, Xia HH, et al. Activation of the caspase-8/Bid and Bax pathways in aspirin-induced apoptosis in gastric cancer. *Carcinogenesis*. 2005;26(3):541–546.
53. Shibata MA, Iinuma M, Morimoto J, et al. alpha-Mangostin extracted from the pericarp of the mangosteen (Garcinia mangostana Linn) reduces tumor growth and lymph node metastasis in an immunocompetent xenograft model of metastatic mammary cancer carrying a p53 mutation. *BMC Med*. 2011;9:69.
54. Bouchard VJ, Rouleau M, Poirier GG. PARP-1, a determinant of cell survival in response to DNA damage. *Exp Hematol*. 2003;31(6):446–454.

55. Yoon JS, Kasin Yadunandam A, Kim SJ, Woo HC, Kim HR, Kim GD. Dieckol, isolated from Ecklonia stolonifera, induces apoptosis in human hepatocellular carcinoma Hep3B cells. *J Nat Med*. 2013;67(3):519–527.
56. Strzalka W, Ziemienowicz A. Proliferating cell nuclear antigen (PCNA): a key factor in DNA replication and cell cycle regulation. *Ann Bot*. 2011;107(7):1127–1140.
57. Mohan S, Abdul AB, Abdelwahab SI, et al. Typhonium flagelliforme induces apoptosis in CEMss cells via activation of caspase-9, PARP cleavage and cytochrome c release: Its activation coupled with G0/G1 phase cell cycle arrest. *J Ethnopharmacol*. 2010;131(3):592–600.
58. Park HS, Park KI, Lee DH, et al. Polyphenolic extract isolated from Korean Lonicera japonica Thunb. induce G2/M cell cycle arrest and apoptosis in HepG2 cells: involvements of PI3K/Akt and MAPKs. *Food Chem Toxicol*. 2012;50(7):2407–2416.
59. Yang F, Sun X, Shen J, et al. A recombined protein (rSj16) derived from Schistosoma japonicum induces cell cycle arrest and apoptosis of murine myeloid leukemia cells. *Parasitol Res*. 2013;112(3):1261–1272.
60. Khan MA, Chen HC, Wan XX, et al. Regulatory effects of resveratrol on antioxidant enzymes: a mechanism of growth inhibition and apoptosis induction in cancer cells. *Mol Cells*. 2013;35(3):219–225.
61. Pozo-Guisado E, Alvarez-Barrientos A, Mulero-Navarro S, Santiago-Josefat B, Fernandez-Salguero PM. The antiproliferative activity of resveratrol results in apoptosis in MCF-7 but not in MDA-MB-231 human breast cancer cells: cell-specific alteration of the cell cycle. *Biochem Pharmacol*. 2002;64(9):1375–1386.
62. Xiao D, Herman-Antosiewicz A, Antosiewicz J, et al. Diallyl trisulfide-induced G(2)-M phase cell cycle arrest in human prostate cancer cells is caused by reactive oxygen species-dependent destruction and hyperphosphorylation of Cdc25C. *Oncogene*. 2005;24(41):6256–6268.
63. Naugler WE, Karin M. NF-κB and cancer-identifying targets and mechanisms. *Curr Opin Genet Dev*. 2008;18(1):19–26.
64. Verfaillie T, Garg AD, Agostinis P. Targeting ER stress induced apoptosis and inflammation in cancer. *Cancer Lett*. 2013;332(2):249–264.
65. Elmore S. Apoptosis: a review of programmed cell death. *Toxicol Pathol*. 2007;35(4):495–516.
66. Fan TJ, Han LH, Cong RS, Liang J. Caspase Family Proteases and Apoptosis. *Acta Bioch Bioph Sin (Shanghai)*. 2005;37(11):719–727.
67. Deveraux QL, Reed JC. IAP family proteins – suppressors of apoptosis. *Gene Dev*. 1999;13(3):239–252.
68. Chai J, Du C, Wu JW, Kyin S, Wang X, Shi Y. Structural and biochemical basis of apoptotic activation by Smac/DIABLO. *Nature*. 2000;406(6798):855–862.
69. Srinivasula SM, Hegde R, Saleh A, et al. A conserved XIAP-interaction motif in caspase-9 and Smac/DIABLO regulates caspase activity and apoptosis. *Nature*. 2001;410(6824):112–116.
70. Mosser DD, Caron AW, Bourget L, et al. The chaperone function of hsp70 is required for protection against stress-induced apoptosis. *Mol Cell Biol*. 2000;20(19):7146–7159.
71. Isa NM, Abdul AB, Abdelwahab SI, et al. Boesenbergin A, a chalcone from Boesenbergia rotunda induces apoptosis via mitochondrial dysregulation and cytochrome c release in A549 cells in vitro: Involvement of HSP70 and Bcl2/Bax signalling pathways. *Journal of Functional Foods*. 2013;5(1):87–97.
72. Yang W, Ahmed M, Tasawwar B, et al. Combination radiofrequency (RF) ablation and IV liposomal heat shock protein suppression: Reduced tumor growth and increased animal endpoint survival in a small animal tumor model. *J Control Release*. 2012;160(2):239–244.

Supplementary materials

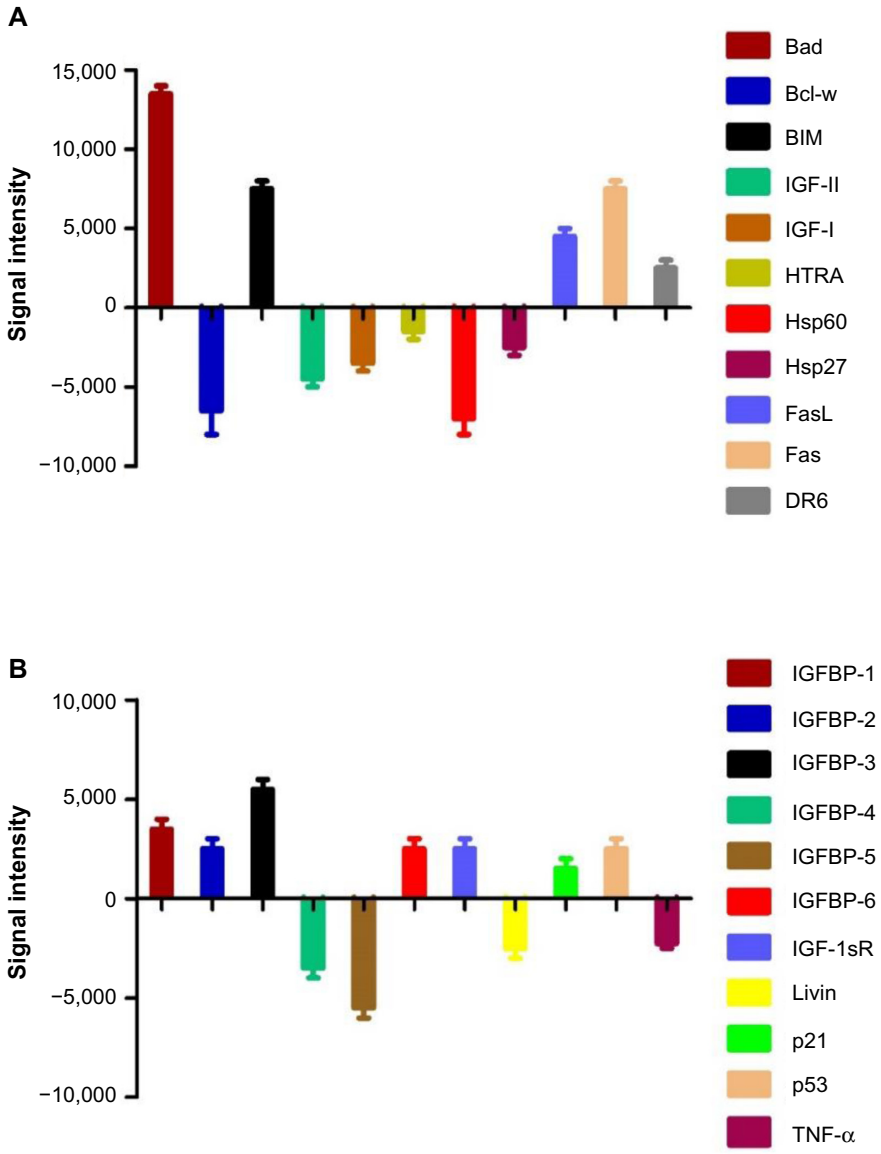

Figure S1 MCF-7 cells were lysed and protein arrays were performed.
Notes: Cells were treated with 20 μg/mL AM and the whole cell protein was extracted. Equal amounts of (300 μg) of protein from each sample were used for the assay (**A** and **B**).
Abbreviations: BAD, Bcl-2-associated death promoter; Bcl-w, Bcl-2-like protein 2; IGF-II, insulin-like growth factor 2; IGF-I, insulin-like growth factor 1; HTRA, high temperature requirement A; Hsp70, heat shock protein 70; Hsp27, heat shock protein 27; FasL, Fas ligand protein; Fas, Fas receptor protein; DR6, death receptor 6; IGFBP, insulin-like growth factor binding protein; Livin, melanoma/kidney inhibitor of apoptosis protein; p21, cyclin-dependent kinase; p53, tumor suppressor p53; TNF-α, tumor necrosis factor alpha; AM, α-Mangostin.